Thermal Science and Engineering (2020) Volume 3 Issue 1
doi:10.24294/tse.v3i1.1498

ORIGINAL RESEARCH ARTICLE

Obtaining a model for the determination of the average condensation heat transfer coefficient in ACC systems

Yanán Camaraza-Medina[1]*, Oscar Miguel Cruz-Fonticiella[2], Osvaldo Fidel García-Morales[3]

[1] *Provincial Freight Dispatching, Matanzas Power Company, Matanzas, Cuba. E-mail: ycamaraza1980@yahoo.com*

[2] *CEETA, Universidad Central de las Villas, Villa Clara, Cuba.*

[3] *College of technical sciences, Universidad de Matanzas, Matanzas, Cuba.*

ABSTRACT

This work presents the results of the continuity of the research process carried out in the Energy Studies ter belonging to the Faculty of Technical Sciences of the University of Matanzas, which involves the establishment of a dimensionless model to determine the average condensation heat transfer coefficient of Air Coleed Condenser (ACC) systems in straight and inclined tubes. The research consists in obtaining in an analytical way the solution of the differential equation of the velocity profile, considering that condensation is of pellicular type, finally the empirical condition of Roshenow is combined with the theoretical solution to generate a numerical expression that allows obtaining with a 15.2% of deviation in 2,192 tests, a value of the average coefficient of heat transfer by condensation very similar to the one obtained with the use of the most referenced model in the consulted literature, the empirical model of Chato.

Keywords: Transfer Roshenow Correction; Heat Transfer Coefficient; Condensation

ARTICLE INFO

Received: 12 March 2020
Accepted: 10 May 2020
Available online: 29 May 2020

1. Introduction

In many heat transfer processes involving saturated steam, it changes into the liquid state through the condensation mechanism. This phenomenon occurs when the vapor comes in contact with a surface at a lower temperature[2,12].

It is known from thermodynamics that when the temperature of a liquid at a specific pressure is raised to the saturation temperature Tsat, boiling occurs. Similarly, when the temperature of a vapor is reduced to Tsat, condensation occurs.

As under equilibrium conditions, the temperature remains constant during the phase transition at a fixed pressure, large amounts of heat can be transferred, due to the high value of the latent heat of vaporization (r_LV) released or absorbed during condensation, essentially at constant temperature. However, in practice it is necessary to maintain some difference between the surface temperature TP and Tsat to have effective heat transfer. Typically, the heat transfer coefficients α associated with condensation are much higher than those found in other forms of convection processes that relate to a single phase[4,6,8,11]. The condensation process requires a cooling agent that is capable of absorbing the enthalpy of the working agent. As the enthalpy of phase change turns out to have a high value (e.g. that of water is 2.58 × 103 kJ/kg at 43.7 ºC and 0.009 MPa), so the average heat transfer coefficients will also turn out to be large. In most industrial applications, both the liquid and vapor phases are concurrent to the same heat transfer equipment.

Thus heat transfer at the interface between liquid and vapor is in essence a convection process, but it is often complicated by a regular interface, such as that produced by bubbles or droplets.

In the overwhelming majority of the available sources consulted, the unified criterion on the use of Chato's expression for obtaining the average heat transfer coefficient by condensation inside horizontal pipes coincides. However, the Chato equation has as a drawback that its generalization uses experimental points of different fluids, including water, although most of them are related to refrigerants. Another drawback of Chato's expression is that it is limited by the velocity of the working agent, being valid only for Reynolds numbers lower than 35,000, thus avoiding operation in the stratified zone, with the consequent danger of condensate stagnation inside the tube. This drawback is partially eliminated in inclined pipes, provided that the flow normals and gravitational forces coincide. The Chato equation considers that the steam has a negligible velocity, so it does not influence the heating of the stratified liquid at the bottom of the pipe, nor does it exert any drag force on it.

Roshenow generalized available experimental data reported by several authors[6,9,10] and created an empirical correction named in his honor, Roshenow's empirical correction, which allows to affect the latent heat to take into account the effect of steam subcooling and steam entrainment, and demonstrated that the use of his correction in the Nusselt equation allows a slight increase in the accuracy of the results obtained. This improvement in accuracy is whithin the range of ± 2%[4,7].

This drawback of the Chato equation was partially solved by Shah and his collaborators[3,9]. These authors generated a model that allows determining the dimensionless Nusselt number, combining the quantities corresponding to the heat flow in the liquid phase by means of the Dittus-Boelter equation and the equation obtained by Nusselt through his simplifying hypotheses for the condensation of a pure vapor. However, Shah's equation gives results with poor accuracy in condensing media that are close to the liquid state, although it does take into account the effect of vapor entrainment provided by the Roshenow correction.

More modern criteria provided by Martineli and Brender[1,2,4,12] subdivide condensation into 4 basic groups, and attribute generalized calculation expressions specifically for each particular zone. However, in the plugged zone, the Dobbson equation which is the most recommended can generate errors that can reach up to 30%, which is eventually solved with the application of the Roshenow correction.

This problem encouraged the authors to create a calculation methodology that takes into account the effect of vapor entrainment and liquid subcooling, and that is as accurate as the expression Chato equation most recommended and referenced in the specialized literature on the subject[1,5,12].

To meet this objective, a combination of the differential relation of the velocity profile inside a tube and the solution of the differential equation of the temperature distribution was carried out. The theoretical solution obtained is subsequently affected by the empirical Roshenow correction. Although the primary results obtained are provided here, the authors continue to refine the model in a futuristic attempt to decrease the correlation errors with respect to available experimental data and to reduce the mathematical complexity of the obtained relationship.

2. Theoretical foundation

2.1 Condensing elements in ACC systems

Heat exchange is a decisive process in the efficiency of the cycle. Approximately 90% of the heat extracted in a power cycle is done through the condensing system. The waste heat coming from the steam turbine is released to the atmosphere from the cooling system, which, depending on the ambient conditions performs this exchange from water circulation systems or direct cooling with the environment[1,4,11,12]. An example of an A-shaped finned tube air-cooled steam condenser unit is shown schematically in **Figure 1**.

A heat exchanger requires a certain temperature gradient for heat transfer to take place. The air condenser is an air-water heat exchanger, which undergoes the same treatment as a classical condenser, where the heat extracted by the air is equal to the heat removed from the fluid to be condensed. The heat released by the flow to be condensed can be determined by the variation of enthalpies that the fluid undergoes, according to the following expression:

$$Q = m_{agua}\left(h_{cond} - h_{fluid}\right) \quad \text{(W)} \tag{1}$$

Where,

m_{Agua} is the steam flow at the turbine outlet, in *kg/s*

h_{cond} is the enthalpy of the fluid at turbine outlet

h_{fluid} is the enthalpy of the fluid at the outlet of the capacitor

The heat absorbed by the air from the fluid is determined by the relationship:

$$Q = m_{aire}Cp\left(T_h - T_{TBS}\right) \quad \text{(W)} \tag{1}$$

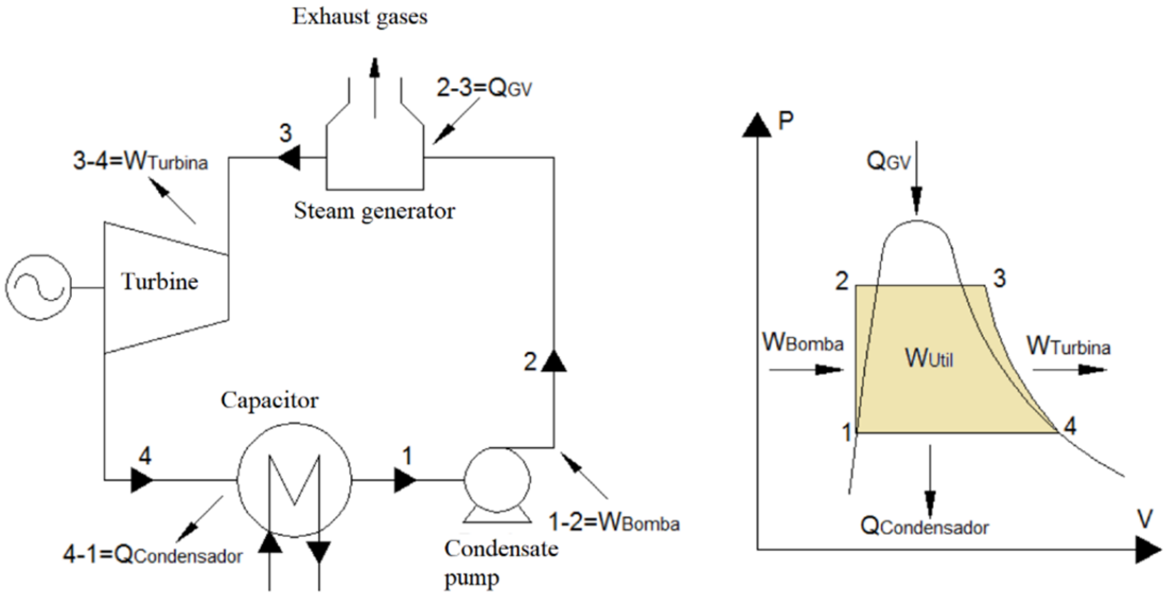

Figure 1. Basic representation of CTE installation including ACC system.

Where m_{aire} is the air flow in *kg/s.*

Cp is the specific heat of the air at the turbine outlet temperature (T_h) and dry bulb temperature (T_{TBS}).

In other words, equations (1) and (2) are the classical energy balance equations.

It's the derivation of an equation for the determination of the average heat transfer coefficient in ACC systems.

In power generating plants and in processing industries using ACC systems, condensation is carried out in an inclined tube bundle. The buoyancy force exerted by the liquid on the tube surface is given by $(\rho_L - \rho_V)g\ sen\,\theta$, which is reasonable, as the tube surface is not flat but curved.

This buoyancy force follows the approximation given by a tangent line to the tube surface, which is generated by the trajectory from the upper part to the lower part, as shown in **Figure 2**.

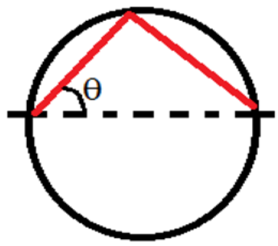

Figure 2. Basic representation of the angle and approximation taken in the present material for the curvature of the tube surface.

Therefore, the angle θ is measured from the top of the tube. The differential equation of the velocity distribution $V(y)$ through the thin film, for any specific value x considering $\Delta y = 0$ is given by the following expression[6,8,10,11]:

$$\mu_L \frac{\partial^2 V}{\partial y^2} + \left(\rho_L + \rho_V\right)g = 0 \tag{2}$$

The differential equation (3) is now affected by the term *sen θ* due to the presence of the aforementioned inclination in the pipe wall, therefore the expression (3) is transformed to the following form[1,3,5,12]:

$$\mu_L \frac{\partial^2 V}{\partial y^2} + (\rho_L + \rho_V) gsen\theta = 0$$

(3)

The differential equation (4) is a differential equation of velocity distribution. In this case, for any particular value of *x*, two boundary conditions are required to solve the velocity *V*(*y*) through the film. On the wall the no-slip condition of the actual fluid is taken, hence:

$$y = 0 \text{ and } V = 0$$

(4)

At the film surface, vapor entrainment is assumed to be minimal. If film thickness is taken, the required boundary condition will then be given by:

$$y = \delta \quad ; \quad \frac{\partial V}{\partial y} = 0$$

(5)

The film thickness $\delta(x)$ is a function yet to be determined. The condition of negligible or negligible vapor entrainment is valid on many occasions when the vapor velocity is not too large. Integrating the differential equation (4) gives:

$$\frac{\partial V}{\partial y} = -\frac{(\rho_L - \rho_V) gsen\theta}{\mu_L} + C_1$$

(6)

Introducing in equation (7) the boundary condition expressed in expression (6) we have that:

$$0 = -\delta \frac{(\rho_L - \rho_V) gsen\theta}{\mu_L} + C_1$$

(7)

By subtracting in (8) the constant of integration C_1 and substituting again we have that:

$$\frac{\partial V}{\partial y} = \frac{(\rho_L - \rho_V) gsen\theta}{\mu_L} (\delta - y)$$

(8)

Integrating again the differential equation (9) we obtain:

$$V = \frac{(\rho_L - \rho_V) gsen\theta}{\mu_L} \left(\delta y - \frac{y^2}{2} \right) + C_2$$

(9)

Based on the boundary conditions given in (6), by applying these boundary conditions in (10), it can be concluded that $C_2 = 0$. Rearrange equation (10) to obtain:

$$V = \delta^2 \frac{(\rho_L - \rho_V) gsen\theta}{\mu_L} \left(\frac{y}{\delta} - \frac{1}{2} \left(\frac{y}{\delta} \right)^2 \right)$$

(10)

Relationship (11) indicates that the velocity profile *V*(*y*) is parabolic. The velocity will reach a maximum over the film surface when $y = \delta$. Substituting this condition in (11), the maximum velocity can be determined[2,4,6]:

$$V_{Max} = \delta^2 \frac{(\rho_L - \rho_V) gsen\theta}{2\mu_L} = \frac{g\delta^2 sen\theta}{2\nu_L} \frac{(\rho_L - \rho_V)}{\rho_L}$$

(11)

By establishing a check of the maximum velocity over the film surface in an inclined tube with the same maximum velocity condition for a vertical surface, identical solutions are obtained except that the former is affected by *sen θ*, caused by the curvature of the surface and the inclination of the tubes. The condensate mass flow per unit film width on vertical and inclined surfaces are also identical[1,12], and remember that they must be affected by *sen θ*, therefore they meet:

$$G = \frac{\rho_L (\rho_L - \rho_V) gsen\theta\delta^3}{3\mu_L} = \frac{(\rho_L - \rho_V) gsen\theta\delta^3}{3\nu_L}$$

(12)

Therefore, the number of film Re is given by:

$$\text{Re} = \frac{4}{3} \frac{(\rho_L - \rho_V) gsen\theta\delta^3}{\rho_L \nu_L^2}$$

(13)

Considering that the length of the tube is much larger than its diameter, and that the process is assumed to be stationary, then the temperature distribution can be treated simplistically as one-dimensional, therefore, according to O'Donovan *et al.*[7] and Chen *et al.*[9], the differential equation of temperature distribution is simplified as:

$$\frac{\partial^2 T}{\partial y^2} = 0$$

(14)

To integrate the differential equation (15), two boundary conditions are required. The continuity of the temperature at the film surface requires that $T = T_{sat}$ (T_{sat} is the saturation temperature corresponding to the vapor pressure *p*), therefore, the first boundary condition is given by:

$$y = \delta \quad ; \quad T = T_{Sat}$$

(15.a)

As a second boundary condition it is assumed that the wall is isothermal at temperature T_p, therefore:

$$y = 0 \quad ; \quad T = T_P$$

(15)

Integrating the differential equation **(15)** twice leads to:

$$T = y \cdot C_1 + C_2$$

(16)

Introducing in (17) the boundary conditions given in (15.a) and (16), the following is obtained:

$$T - T_P = \frac{y}{\delta}\left(T_{Sat} - T_P\right)$$

(17)

Relationship (18) is a linear temperature profile, since the problem is identical to that of conduction through a flat plate. Therefore, the heat flux per unit area to the wall is simply the flux per unit area through the film, i.e., the heat flux per unit area through the film, that is:

$$\lambda_L \left.\frac{\partial T}{\partial y}\right|_P = \frac{Q}{F} = \lambda_L \frac{\left(T_{Sat} - T_P\right)}{\delta}$$

(18)

The local heat transfer coefficient a is defined as the ratio that exists between the heat flux per unit area and the temperature difference across the film, hence[8,10,11]:

$$\alpha = \frac{q}{\left(T_{Sat} - T_P\right)} = \frac{\lambda_L \left.\frac{\partial T}{\partial y}\right|_P}{\left(T_{Sat} - T_P\right)} = \frac{\lambda_L}{\delta}$$

(19)

In equation (20) q has been assumed positive for condensation, therefore the energy balance can be written as:

$$q = \lambda_L \left.\frac{\partial T}{\partial y}\right|_P = \frac{\lambda_L\left(T_{Sat} - T_P\right)}{\delta} = \left(r_{LV}\right)\frac{dG}{dx}$$

(20)

By specifying the boundary condition on the wall, we obtain the expression for an isothermal wall at T_p. By subtracting the thickness δ in equation (21)

$$\delta = \sqrt[3]{\frac{3}{4}\frac{\rho_L \nu_L^2}{\left(\rho_L - \rho_V\right)g}\frac{\mathrm{Re}}{sen\theta}}$$

(21)

Substituting equation (21), (13) and (14) into (21), we obtain that:

$$\frac{2\lambda_L\left(T_{Sat} - T_P\right)d}{\mu_L\left(r_{LV}\right)}\left(\frac{4}{3}\frac{\left(\rho_L - \rho_V\right)g}{\rho_L \nu_L^2}\right)^{1/3} sen^{1/3}\theta \, d\theta = \mathrm{Re}^{1/3}\, d\,\mathrm{Re}$$

(23)

Integrating in (23) with $Re = 0$ at $\theta = 0$ and $\mathrm{Re} = \mathrm{Re}_\pi$ at $\theta = \pi$, we can obtain:

$$\mathrm{Re}_\pi = \left[\left(\frac{4}{3}\right)\frac{2\lambda_L\left(T_{Sat} - T_P\right)d}{\mu_L\left(r_{LV}\right)}\left(\frac{4}{3}\frac{\left(\rho_L - \rho_V\right)g}{\rho_L \nu_L^2}\right)^{1/3}\int_0^\pi sen^{1/3}\theta \, d\theta\right]^{3/4}$$

(24)

It's an interesting and important observation. Preference was given to employing Re rather than thickness δ as the independent variable, and the explanation is simple. The Re number is worth zero at $\theta = 0$ because, by symmetry, the mass flow rate is zero at the top of the tube, while the film thickness at $\theta = 0$ is finite and unknown[1,3,5,7].

An overall energy balance over the middle of the tube gives the average heat transfer coefficient, so that:

$$\bar{\alpha}\left(\frac{\pi d}{2}\right)\left(T_{Sat} - T_P\right) = G_\pi\left(r_{LV}\right) = \frac{\mu_L\left(r_{LV}\right)\mathrm{Re}_\pi}{4}$$

(22)

Substituting the value of Re p in equation (24) and rearranging, we obtain:

$$\bar{\alpha} = \left(\frac{4}{3\pi}\right)\left(\frac{1}{2}\right)^{1/4}\left(\int_0^\pi sen^{1/3}\theta \, d\theta\right)^{3/4}\left(\frac{\left(\rho_L - \rho_V\right)g\left(r_{LV}\right)\lambda_L^3}{\nu_L\left(T_{Sat} - T_P\right)d}\right)^{1/4}$$

(23)

The integral present in equation (26) can be solved by the known integration techniques to obtain:

Therefore,

$$\int_0^\pi sen^N x \, dx = \frac{\sqrt{\pi}}{2}\frac{\Gamma\left(\frac{n}{2} + 0{,}5\right)}{\Gamma\left(\frac{n}{2} + 1\right)} \quad para \;\; N > -1$$

(24)

An interesting solution is reached in (27), because $\Gamma\left(\frac{n}{2} + 0.5\right)$ and $\Gamma\left(\frac{n}{2} + 1\right)$ are gamma functions, with their particularities and special properties. In short, for $n = 1/3$, it must be that:

$$\Gamma\left(\frac{n}{2} + 0.5\right) = 1.35411793$$

(25)

$$\Gamma\left(\frac{n}{2} + 1\right) = 0.92771933$$

(26)

Substituting (28) and (29) in (27) we obtain:

$$\int_0^{\pi} sen^N x\,dx = \frac{\sqrt{\pi}}{2}\frac{\Gamma\left(\frac{n}{2}+0,5\right)}{\Gamma\left(\frac{n}{2}+1\right)} = \frac{\sqrt{3.1415926}}{2}\frac{1.35411793}{0.92771933} = 1.293554 \quad (27)$$

Therefore

$$\int_0^{\pi} sen^{1/3}\theta\,d\theta = 2\int_0^{\pi/2} sen^{1/3}\theta\,d\theta = 2(1.293554) = 2.5871095 \quad (28)$$

Substituting (31) in (26) we obtain:

$$\overline{\alpha}_{Horiz} = 0.923\left(\frac{(\rho_L-\rho_V)g(r_{LV})\lambda_L^3}{\nu_L(T_{Sat}-T_P)d}\right)^{0.25} \quad (29)$$

The latent heat (r_{LV}) at (32) is replaced by the Roshenow correction (r_{LV})", which states that when there is a possibility of liquid subcooling, the latent heat should be affected as follows[2,4,6]:

$$(r_{LV})" = (r_{LV}) + \frac{3}{8}Cp_L(T_{Sat}-T_P) \quad (30)$$

It is also known that the kinematic viscosity is equal to the quotient of the dynamic viscosity and the density; therefore, applying this criterion and substituting (33) in (32) we can get:

$$\overline{\alpha} = 0.923\left(\frac{\lambda_L^3\rho_L(\rho_L-\rho_V)g\left(r_{LV}+\frac{3}{8}Cp_L(T_{Sat}-T_P)\right)}{\mu_L(T_{Sat}-T_P)d}\right)^{0.25} \quad (31)$$

Finally, since it is an inclined surface, and the acceleration of gravity is present in the denominator, it is affected by the sine of the angle (ϕ) formed with the horizontal plane in the form of product, and finally:

$$\overline{\alpha} = 0.923(Sen(\theta))^{0.25}\left(\frac{\lambda_L^3\rho_L(\rho_L-\rho_V)g\left(r_{LV}+\frac{3}{8}Cp_L(T_{Sat}-T_P)\right)}{\mu_L(T_{Sat}-T_P)d}\right)^{0.25} \quad (32)$$

In expression (35): ρ_L is the density of the saturated liquid in kg/m^3; ρ_V is the density of saturated vapor in kg/m^3; r_{LV} is the latent heat in *kJ/kg*; Cp_L is the specific heat of the liquid in *kJ/kg°C*; T_{Sat} is the saturation temperature in *°C*; T_P is the temperature of the pipe wall in $°C_{TUVO}$; μ_L is the dynamic viscosity of the liquid in $Pa{\cdot}s$; *d* is the internal diameter of the tubes in m.

The Chato equation described by the following expression[12]:

$$Nu = \frac{\alpha d}{\lambda_L} = 0.023\,\mathrm{Re}_L^{0.8}\,\mathrm{Pr}_L^{0.4}\left[1+\frac{2.22}{\sqrt{\rho_V/\rho_L}\cdot\left(\frac{1-x}{x}\right)^{0.9}(\mu_L/\mu_V)^{0.1}}\right] \quad (33)$$

In expression (36) the dimensionless numbers of Re and Pr are determined as a function of the liquid state parameters, while x is the vapor quality.

Experimental validation of the new model determines the average condensation heat transfer coefficient.

A large group of experimental points for the condensation of water vapor and other refrigerants (R-22, R-134a, R-410, etc.) is provided[1], from which were arbitrarily taken a total of 2,192 values that are located in the intervals $10^3 \leq \mathrm{Re}_L \leq 2.5\cdot10^6$ covering vapor qualities from 0 to 1, the vapor temperatures are between $32 \leq T \leq 520°C$, and pressures cover the range $0.005 \leq T \leq 20.8MPa$. In all cases where there is subcooling the liquid temperature is included in the intervals $0.72\cdot T_{Sat} \leq T_{Lsub} < T_{Sat}$, while the friction factor f is evaluated for the medium in two phases (liquid + vapor) by the well-known Martinelli equation[1,12]. In the validation of the obtained model the wall temperature is taken as the arithmetic mean of the temperatures at the inlet and outlet of the pipe. Using the professional software TkSolver 5.0, a comparative function can be run, setting a tolerance value (permissible error) equal to 10^{-6} and using the IAPWS Formulation 1995 for the Thermodynamic Properties of Ordinary Water Substance for General and Scientific Use for the determination of the physical properties of water. The results are expressed in Cartesian coordinates. The complex number is the coordinate axis $Log\left(Re\cdot Pr\cdot\frac{f}{8}\right)$, and the quotient is the coordinate axis of accisas (%error/150). The error committed with the use of equation (35) tends to decrease as the value of the complex $Log\left(Re\cdot Pr\cdot\frac{f}{8}\right)$ increases, finding for $Log\left(Re\cdot Pr\cdot\frac{f}{8}\right) = 3.5$ an average error equal to 12.86% and for $Log\left(Re\cdot Pr\cdot\frac{f}{8}\right) = 5.08$ an average error equal to 8.75%. The tests carried out also allow obtaining that the expression (35) correlates in a general way with an average error in the order of ± 15.2% for 84.12% of the available experimental samples, as shown in **Figure 2**.

In **Figure 1** itself, the Chato equation (36) was represented by a continuous red line, which represents approximately the same correlation error pattern as equation (35) in the interval $3.8 \leq Log\left(Re\cdot Pr\cdot\frac{f}{8}\right) \leq 4.05$. However, this parameter becomes more acute outside this interval, reaching the order of $\approx \pm 25\%$ in the zones $3.55 \leq Log\left(Re\cdot Pr\cdot\frac{f}{8}\right) \leq 3.7$ and $4.14 \leq Log\left(Re\cdot Pr\cdot\frac{f}{8}\right) \leq 4.22$.

Table 1. Comparison of the average heat transfer coefficient obtained with (35) and (36) with 3 experimental points

Parameters	α Experimental	α (Chato)	α (Camaraza etal)
Re = 22,000, P = 0.009 MPa X = 0.9, D = 0.032, T_P = 40 ºC	3,028.2	2,522.0 16.71% error	2,816.6 6.98% error
Re = 11,000, P = 0.015 MPa X = 0.92, D = 0.04, T_P = 45 ºC	2,312.1	2,408.9 4.18% error	2,104.1 8.99% error
Re = 33,800, P = 0.018 MPa X = 0.94, D = 0.025, T_P = 50 ºC	4,142.4	3,877.9 6.49% error	4,289.6 3.42% error

Table 1 provides a comparison between the values of the average heat transfer coefficient obtained with the use of equation (36) and the proposed model (35) for 3 experimental values. All coefficients are given in $W/m^2\ ºC$. All the values of Re used in the comparison are less than 35,000, taking into account that for values greater than this dimensionless number the expression (36) is not valid.

Figure 3 plots the correlation errors of expressions (35) and (36).

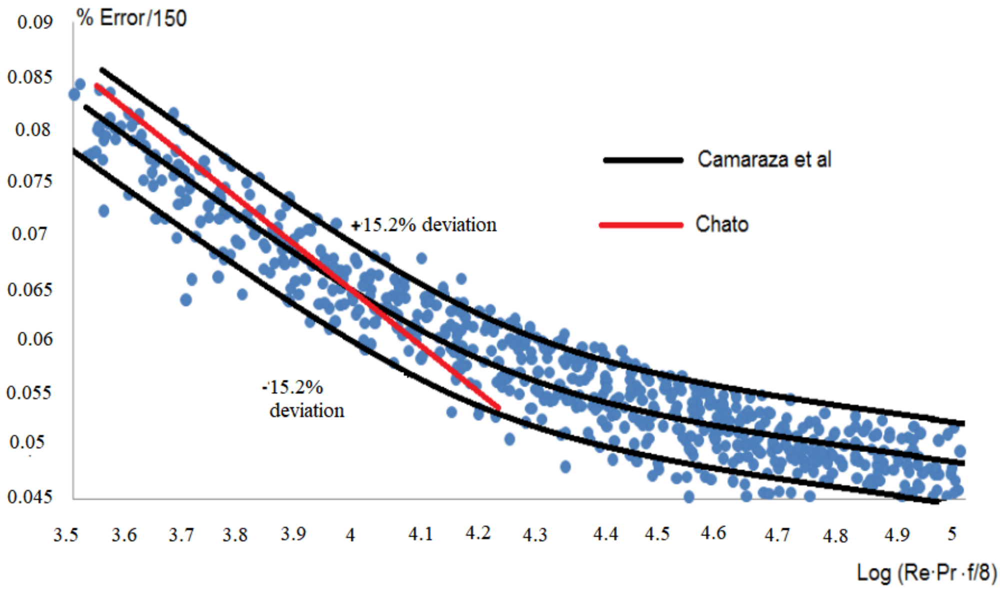

Figure 3. Graphical representation of the correlation errors of expressions (35) and (36).

3. Conclusions

Through analysis, a model for the determination of the average heat transfer coefficient by condensation in ACC system is obtained. The model is suitable for horizontal and inclined straight pipes, and it has a superior fit to the model of greater diffusion in the known literature, i.e. the Chato equation, better fitting equation (36) with existing experimental data within the range of $3.55 \leq Log\left(Re \cdot Pr \cdot \frac{f}{8}\right) \leq 3.7$ and $4.14 \leq Log\left(Re \cdot Pr \cdot \frac{f}{8}\right) \leq 4.22$, not in the interval $3.8 \leq Log\left(Re \cdot Pr \cdot \frac{f}{8}\right) \leq 4.05$. The new model obtained is valid for a greater interval of the number of Re $10^3 \leq Re_L \leq 2.5 \cdot 10^6$, unlike (36) which is only valid for $Re_L < 3.5 \cdot 10^4$ and correlates in general with an average error ± 15.2% of the order of 84.12% of the available experimental samples, surpassing the 18.2% error attributed to Chato's model, which is coincident with the initial criteria that founded the investigation, considering that the objectives of the same have been fulfilled. The authors consider that possible adjustments with new experimental quantities could reduce the correlation error in the interval $3.8 \leq Log\left(Re \cdot Pr \cdot \frac{f}{8}\right) \leq 4.05$ effectively.

The new model obtained responds to the following expression:

$$\bar{\alpha} = 0{,}923(Sen(\phi))^{0{,}25}\left(\frac{\lambda_L^3 \rho_L(\rho_L - \rho_V)g\left(r_{LV} + \frac{3}{8}Cp_L(T_{Sat} - T_P)\right)}{\mu_L(T_{Sat} - T_P)d}\right)^{0{,}25}$$

Conflict of interest

The authors declared that they have no conflict of interest.

References

1. Watson R, Chapman K. Radiant heating and cooling handbook. New York: McGraw-Hill; 2014. p. 657.
2. Dorao CA, Fernandino M. Dominant dimensionless groups controlling heat transfer coefficient during flow condensation inside tubes. International Journal of Heat and Mass Transfer 2017; 112: 465–479.
3. Kröger DG. Air-cooled heat exchanger and cooling tower. Oklahoma: Pennwell Corporation; 2012. p. 502.
4. Heyns JA. Performance characteristics of an air-cooled steam condenser with a hybrid dephlegmator. Journal of the South African Institution of Mechanical Engineering 2012; 28: 31–36.
5. Deziani M, Rahmani K, Mirrezaei Roudaki SJ, *et al*. Feasibility study for reducing water evaporative loss in power plant cooling tower by using air heat exchanger with auxiliary fan. Desalination 2015; 406: 119–124.
6. Mortensen K. Improved performance of an air cooled condenser (ACC) using SPX wind guide technology at coal-based thermoelectric power plants. California: SPX Technology; 2013. p. 28–52.
7. O'Donovan A, Grimes R, Moore J. The influence of the steam-side characteristics of a modular air-cooled condenser on CSP plant performance. Energy Procedia 2017; 49: 1450–1459.
8. Yao E, Wang H, Wang L, *et al*. Thermo-economic optimization of a combined cooling, heating and power system based on small-scale compressed air energy storage. Energy Conversion and Management 2017; 118: 377–386.
9. Chen L, Yang L, Du X, *et al*. A novel layout of air-cooled condensers to improve thermo-flow performances. Applied Energy 2016; 165: 244–259.
10. Salimpour MR, Bahrami Z. Thermodynamic, heat transfer analysis and optimization of air-cooled heat exchangers. Heat and Mass Transfer 2011; 47: 35–44.
11. Xiao L, Ge Z, Du X, *et al*. Operation of air-cooling CHP generating unit under the effect of natural wind. Applied Thermal Engineering 2016; 107: 827–836.
12. Camaraza Medina Y. Introducción a la termo transferencia (Spanish) [Introduction to heat transfer printing]. La Habana: Editorial Universitaria; 2017. p. 1341.